

---

# SIMPLIFYING CLIP: UNLEASHING THE POWER OF LARGE-SCALE MODELS ON CONSUMER-LEVEL COMPUTERS

---

**Hongbo Liu**

Tongji  
Univ  
Shanghai

## ABSTRACT

Contrastive Language-Image Pre-training (CLIP) has attracted a surge of attention for its superior zero-shot performance and excellent transferability to downstream tasks. However, training such large-scale models usually requires substantial computation and storage, which poses barriers for general users with consumer-level computers. Motivated by this observation, in this paper we investigate how to achieve competitive performance on only one Nvidia RTX3090 GPU and with one terabyte for storing dataset. On one hand, we simplify the transformer block structure and combine Weight Inheritance with multi-stage Knowledge Distillation (WIKD), thereby reducing the parameters and improving the inference speed during training along with deployment. On the other hand, confronted with the convergence challenge posed by small dataset, we generate synthetic captions for each sample as data augmentation, and devise a novel Pair Matching (PM) loss to fully exploit the distinguishment among positive and negative image-text pairs. Extensive experiments demonstrate that our model can achieve a new state-of-the-art datascale-parameter-accuracy tradeoff, which could further popularize the CLIP model in the related research community.

## 1 Introduction

Pre-trained large image-text foundation models, famous as the contrastive language-image pre-training (CLIP) model [28], have recently drawn considerable attention in the fields of computer vision and natural language processing. These models have demonstrated excellent zero-shot performance and robustness across a wide range of downstream tasks, such as image-text retrieval and classification (Zhu et al. 2023). However, the substantial computational and storage costs for training CLIP-like models impeded their further popularization. For instance, MobileCLIP [33] was trained on 256×A100 GPUs with a global batch size of 65,536, and the corresponding dataset DataCompDR-1B requires 140 TB local storage space. In addition, the huge parameter size (e.g., CLIP-B/16 model [28] consists of 86.2M parameters for the image encoder and 63.4M parameters for the text encoder) contributes to increasing inference latency, which raises challenges for deploying the model on devices with limited computational resources. These shortcomings pose barriers for general users with insufficient computational resources and datasets to engage in the training and deploying of such large-scale models.

In practice, the GPU memory of consumer-level computers typically does not exceed 24GB (e.g., Nvidia RTX3090), while storage capacity could be less than 1TB. In the context of training CLIP-like models under such resource constraints, two primary problems have to be addressed. Firstly, it is imperative to minimize the number of parameters that need training, while retaining existing model knowledge as much as possible. Secondly, small-scale datasets need to be augmented appropriately, and more effective methods need to be developed to fully exploit the internal correlation of image-text pairs within the limited samples.

In this paper, we investigate how to train a lightweight CLIP model using only one RTX3090 GPU and 1TB of storage, thereby popularizing the research of CLIP-like models on consumer-level computers. To this end, we first propose to simplify the traditional transformer block as SAS-P block, together with applying the strategy of weight sharing. Then, by inheriting weights and distilling knowledge from existing models, the number of parameters required for training can be reduced further. In terms of the dataset, we choose the widely used CC12M [1] as a basis. The dataset not only

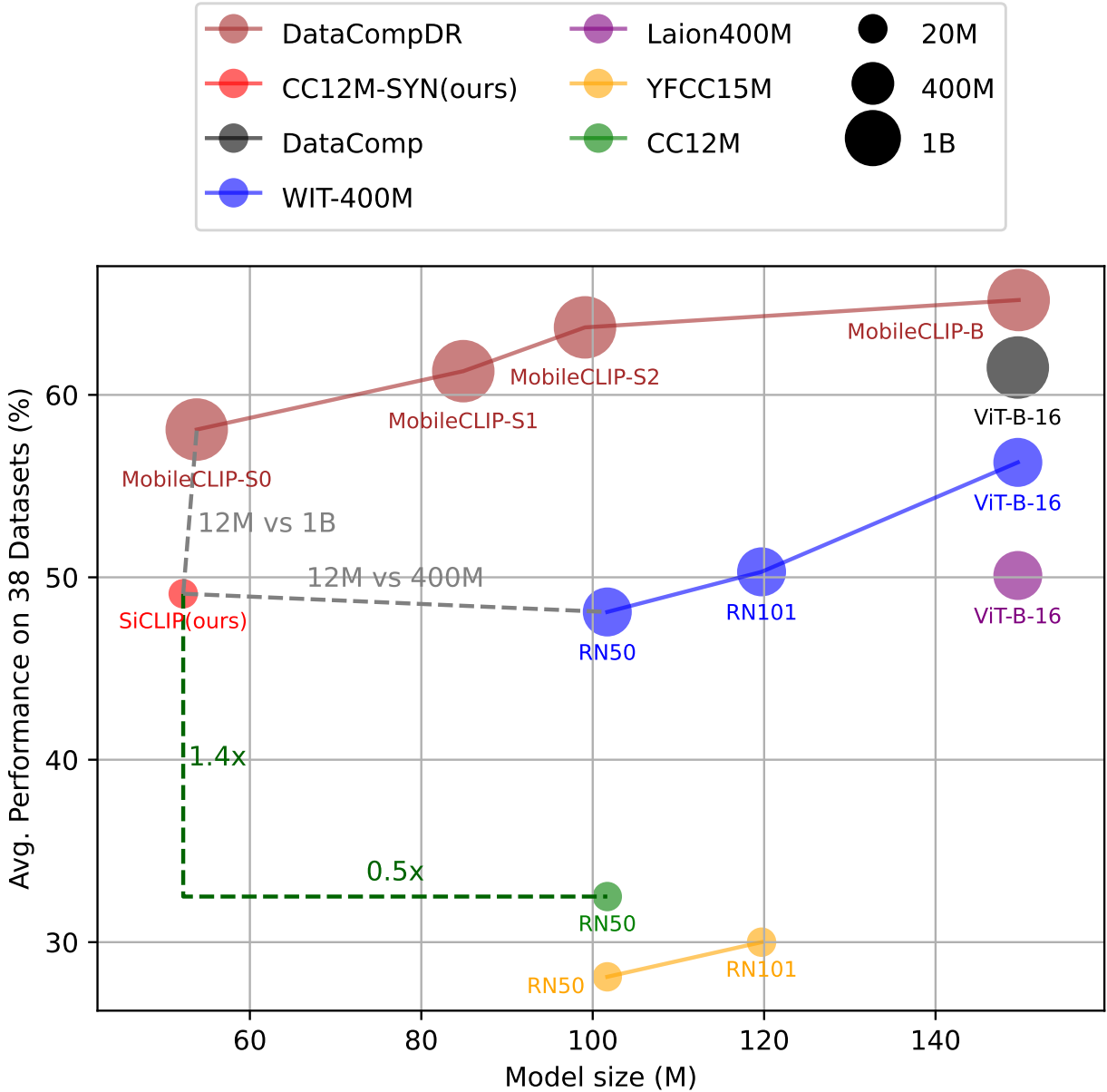


Figure 1: Average zero-shot performance on downstream tasks. Compared to current works, our model achieves competitive performance with a smaller model size while being trained on a small-scale (12M) dataset.

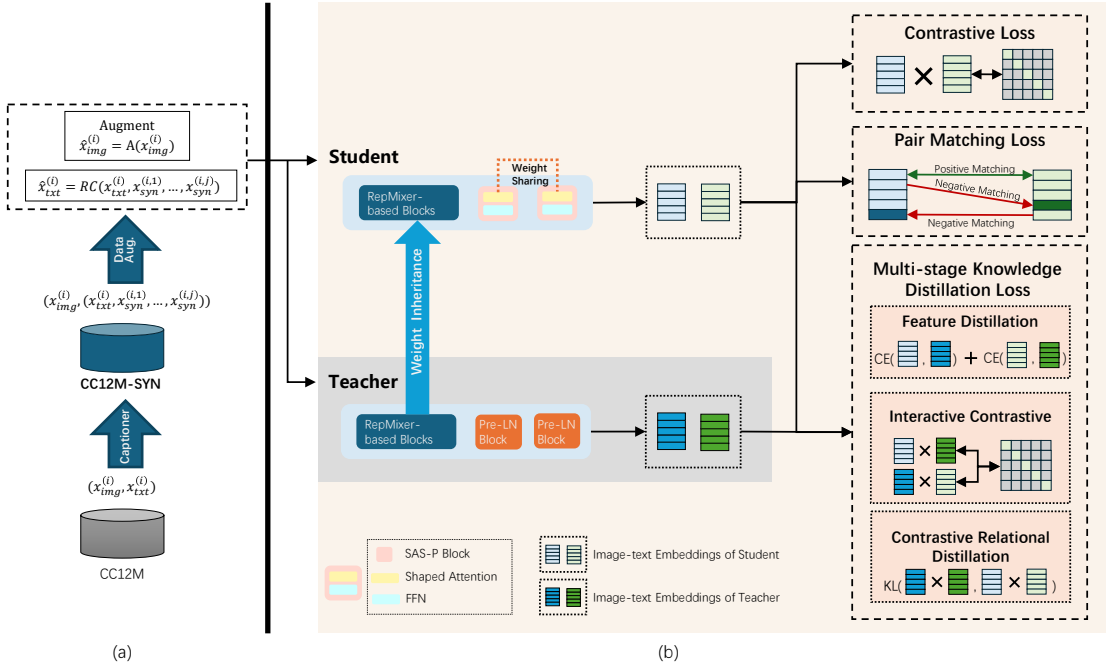
suffers from its small scale but also exhibits low-quality of its labels, which both bring difficulty on convergence of model training process. To address this issue, we enhance each image samples of the CC12M with multiple text labels, creating the new CC12M-SYN. Furthermore, to extract valuable information from such small dataset, we introduce the Pair Matching (PM) loss to help the model capture the distinguishment among positive and negative image-text pairs. These methods significantly improve the convergence speed of model training with our extensive experiments. Finally, through performance comparisons across 38 datasets with several popular approaches (Fig. 1), our proposed SiCLIP framework achieves a new state-of-the-art datascale-parameter-accuracy trade-off.

**Our contributions:** The contributions of this work can be summarized as follows:

- We propose a systematic framework for training lightweight CLIP models on a consumer-level computer, including the dataset construction and the corresponding training procedure, named as SiCLIP. In SiCLIP, both

the computational and storage cost have been reduced, while retaining competitive performance compared to other large-scale models.

- We simplify the CLIP model structure by sharing weights among SAS-P blocks, and combine Weight Inheritance with multi-stage Knowledge Distillation (WIKD), thereby reducing the memory requirements when training and deploying.
- A new loss function called PM loss is devised, which predicts whether an image-text pair is matched or not during training. Coupling with our augmented dataset CC12M-SYN, the PM loss can exploit the distinction among positive and negative image-text pairs. Experimental results show that both the new dataset and PM loss can improve the training efficiency significantly while increasing the dataset size marginally.



## 2 Related Work

### 2.1 Efficient Training for CLIP

Ever since the introduction of CLIP as a large image-text foundation model with impressive zero-shot performance for a wide variety of downstream tasks, there have been a number of works aiming to improve its training efficiency and model size. Examples include fine-grained image-text alignment [42], data augmentation [23, 20, 33], unimodal self-supervision [23, 20], and contrastive learning in image-text-label space [39]. In addition, Zhai et al. [45] propose the pairwise sigmoid loss as a simple alternative to contrastive loss, demonstrating its effectiveness when training with a small batch size. However, it may cause quadratic computational complexity because the matching logits are calculated between all positive and negative image-text pairs. Li et al. [19] use fine-grained image-text matching (ITM) loss as a complement to the contrastive loss, but ITM needs a multi-layer transformer based encoder to encode the multimodal fine-grained features, which is not suitable for lightweight models.

Weight Inheritance (WI) and Knowledge Distillation (KD) [13] based methods are also adopted for efficient training. TinyCLIP [36] trains compact CLIP models via cross-modal affinity mimicking and WI. Yang et al. [38] explore the effectiveness of different KD methods for CLIP training.

Quality of datasets is also important for efficient training. Fang et al. [6] and Gadre et al. [7] have exploited filtering methods to remove noisy samples. However, remaining captions may still not be descriptive enough. Recent works [40, 18] show that synthetic captions generated from a pre-trained captioning model can improve dataset quality.

## 2.2 Simplifying the Transformer Architecture

Following the remarkable success of transformers in a large variety of tasks, recent years have witnessed many efforts to simplify the transformer architecture to increase their training and inference efficiency. Yu et al. [44] demonstrated that the general structure of transformer blocks is more essential for the performance, making it possible to eliminate the attention-based token mixers, which are usually prohibitively expensive due to the quadratic complexity of multi-head self-attention (MHSA) over a long sequence of representations. Besides, previous studies in both CNNs and transformers have shown that shallow layers mainly focus on local patterns while deeper layers tend to capture high-level semantics or global relationships [14, 37, 5], thus it is usually unnecessary to model global relationship by MHSA at the early stages. Based on these facts, Liu et al. [22] proposed a hierarchical transformer, and employed shifted windows to limit self-attention computation to non-overlapping local windows while also allowing for cross-window connection, bringing greater efficiency. In a different line of work, Pan et al. [26] and Guo et al. [9] introduce convolutional layers into early transformer layers. Following these works, Vasu et al. [32] proposed RepMixer as a token mixer, which uses structural reparameterization to lower the memory access cost by removing skip-connections in the network.

As a simple but effective lightweight method, weight-sharing strategy has been employed in many transformer-based models. Dehghani et al. [3] first proposed the idea of reusing the transformer layer for natural language processing tasks with a different motivation: they regard repeated network layers as a complementary way of introducing a recurrent inductive bias to transformers, and it was observed that their method outperforms the vanilla transformer on several tasks. Jaegle et al. [17] adopted the cross-attention layer weight sharing in multimodal pre-training. Hernandez et al. [12] explored sharing different parts of conformer [8] at different levels of granularity with the model size hard-constrained by memory. Most recently, He et al. [10] studied the standard Pre-LN transformer block [34] through signal propagation theory and proposed a simplified parallel structure transformer block equipped with shaped attention [25] as token mixers, named as Simplified Attention Sub-block Parallel (SAS-P), reducing the number of parameters and increasing throughput of the model without performance loss on language downstream tasks. Our work is the first attempt on extending SAS-P into the multi-modal domain, and further simplify it by sharing weights of the token mixers between adjacent blocks.

## 3 Methods

In this section, we first introduce our simplified model structure, which shares weights among SAS-P blocks. Then, we introduce a method called WIKD for efficient training. Next, we introduce a novel loss function, called the pair matching (PM) loss, to further improve the training performance. Finally, we also improve the CC12M dataset, which we use for training our model, by adding synthetic captions to improve data diversity and data quality, with minimal additional storage. The new dataset is called CC12M-SYN. Fig. 2 shows the overall framework of our method.

### 3.1 Simplifying Model Structure by Sharing Weights Among SAS-P Blocks

Our architecture is built upon the state-of-the-art MobileCLIP-S0 model [33], which we enhance in multiple ways. The MobileCLIP-S0 framework features hybrid structures for both the image encoder and text encoder, incorporating a synergistic arrangement of convolution-based and MHSA-based blocks. However, for each MHSA-based block, MobileCLIP-S0 simply adopts the standard Pre-LN block with MHSA as the token mixer [34], as shown in Fig. 3 (left).

We start by reducing the parameters of the skip connections within each Pre-LN block. The presence of these connections causes a bottleneck on memory access and inference speed, and a lightweight MHSA-based block design becomes essential. Moreover, it has been shown that the feed-forward layers can be integrated into the attention module without degrading performance of the transformer layer [31, 24].

The right-hand side of Fig. 3 illustrates SAS-P (He and Hofmann 2024), a simplified parallel transformer block that eliminates skip connection along with the value and projection parameters. It uses shaped attention [25] as its token mixer to prevent signal degradation after removing skip connections, making attention matrices more identity-like to maintain a good signal propagation. The attention matrices of shaped attention are given by:

$$A(X) = \text{Softmax} \left( \frac{1}{\sqrt{d_v}} X W^Q W^{K^T} X^T \right), \quad (1)$$

$$A(X) \leftarrow \alpha I_T + \beta A(X) - \gamma C, \quad (2)$$

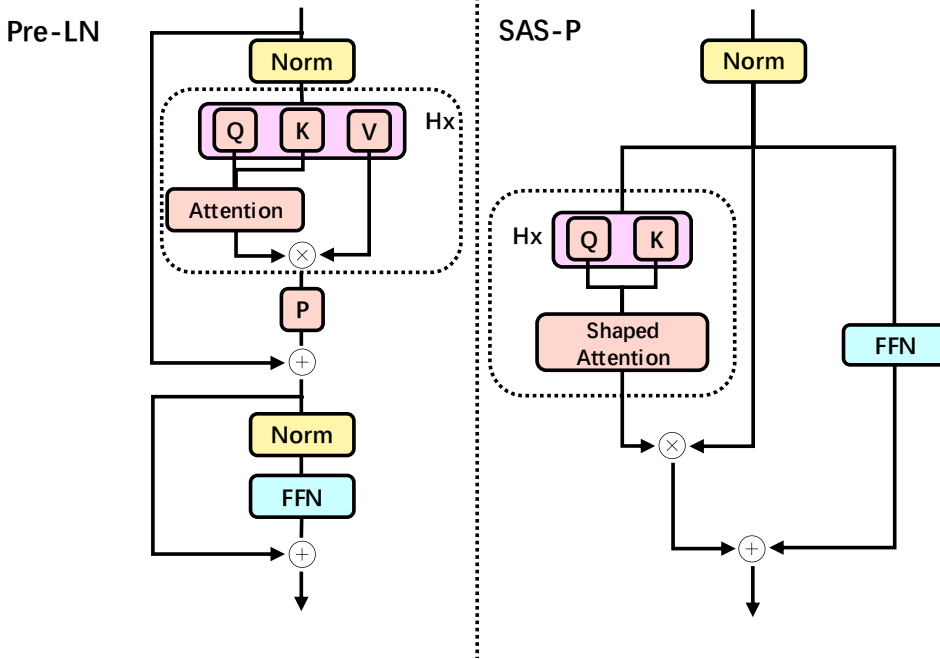


Figure 3: Pre-LN block [34] vs SAS-P block [10]. SAS-P block removes skip connections, value and projection parameters, leading to faster inference speed with fewer parameters than Pre-LN.

where  $X$  denotes the SAS-P input,  $W^Q$  and  $W^K$  are the query and the key matrices,  $d_v$  is the model dimension,  $I_T$  is the identity matrix, and  $\alpha, \beta, \gamma$  are learnable parameters.  $C$  is the center matrix, and each element of  $C$  is set to  $\frac{1}{n}$ , with  $n$  being the number of input tokens. At initialization,  $W^Q$  is set to 0,  $\alpha, \beta, \gamma$  are set to 1, leading to  $\beta A(X) - \gamma C = 0$  and  $A(X) = I_T$ , which is effective for good signal propagation. SAS-P shows impressive performance on several language tasks [10] while achieving faster inference speed with fewer parameters than Pre-LN.

To simplify the model structure further, we evaluate the Jensen-Shannon (JS) divergence between adjacent MHSA-based blocks (see Fig. 4). A low JS divergence implies that weight sharing can be used among these matrices without degrading the performance. Accordingly, before employing KD during training, our ‘student’ model replaces all of the Pre-LN blocks with SAS-P blocks, and apply weight sharing among these blocks. As a result, the image encoder of our model has approximately 14% fewer parameters compared to MobileCLIP-S0, and only 11% of that in OpenAI-B/16 [28].

### 3.2 Weight Inheritance with Multi-Stage Knowledge Distillation (WIKD)

To benefit from small-scale datasets, a widely used paradigm is to employ a task-related pre-trained backbone and add a few task-specific layers [15]. Inspired by the idea of using backbones, we adopt WI [36] to train CLIP on small-scale datasets. In practice, since we modify the MHSA-based blocks of MobileCLIP-S0 structure and keep the RepMixer-based blocks unmodified (which are already efficient), we can directly inherit the weights of these modules from MobileCLIP-S0 which has been well pretrained on a large-scale dataset [33]. In this case, the inherited modules can be seen as the ‘backbone’. Then, we freeze these inherited layers and only train the newly added SAS-P blocks on a much smaller dataset. Applying the above methods can reduce gradient storage, and thus allow us to use a larger batch size to maintain the performance of contrastive learning.

Moreover, we regard our model as a student model of MobileCLIP-S0, and perform multi-stage KD during training, leading to further performance improvement. Specifically, we apply KD on the unimodal feature space (stage 1), contrastive relation space (stage 2), and interactive contrastive space (stage 3). Given a batch of image-text pairs, the student model firstly mimics the image and text feature distributions of the teacher by optimizing feature distillation loss ( $L_{FD}$ ), given by:

$$L_{FD} = \frac{1}{|B|} \sum_{k=1}^{|B|} (||v_k^T - v_k^S||_2^2 + ||t_k^T - t_k^S||_2^2)/2, \quad (3)$$

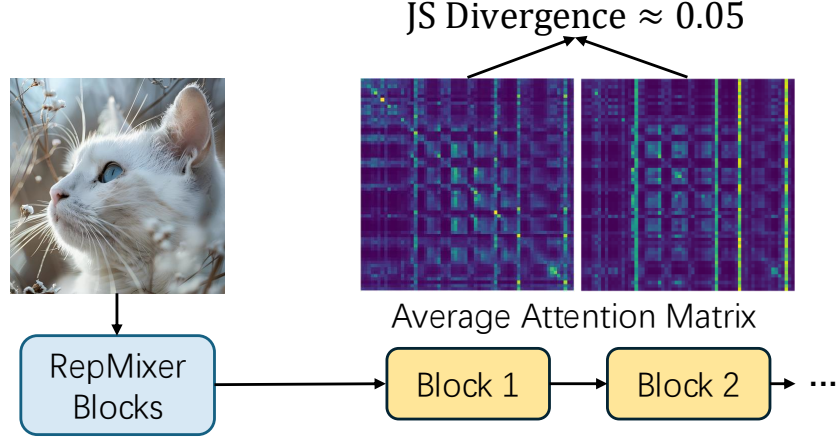


Figure 4: Illustration of JS divergence of the average multi-head attention matrices between adjacent blocks.

where  $(v_k^T, t_k^T)$  and  $(v_k^S, t_k^S)$  represent (image, text) features of the teacher and student models, respectively, where  $B$  is the batch size. Then, it computes the contrastive relational distillation loss ( $L_{\text{CRD}}$ ) and interactive contrastive loss ( $L_{\text{IC}}$ ) to mimic the image-text similarity matrix distributions in contrastive relation space and interactive contrastive space, defined as:

$$L_{\text{IC}_{I \rightarrow T}} = - \sum_{k=1}^{|B|} \log \frac{\exp(v_k^S \cdot t_k^T / \tau)}{\sum_{b=1, b \neq k}^{|B|} \exp(v_k^S \cdot t_b^T / \tau)}, \quad (4)$$

$$L_{\text{IC}_{T \rightarrow I}} = - \sum_{k=1}^{|B|} \log \frac{\exp(t_k^S \cdot v_k^T / \tau)}{\sum_{b=1, b \neq k}^{|B|} \exp(t_k^S \cdot v_b^T / \tau)}, \quad (5)$$

$$L_{\text{IC}} = \frac{1}{2}(L_{\text{IC}_{T \rightarrow I}} + L_{\text{IC}_{I \rightarrow T}}), \quad (6)$$

$$L_{\text{CRD}} = \frac{1}{|B|} \text{KL}(\text{Sim}_T || \text{Sim}_S), \quad (7)$$

where  $\tau$  is a learnable temperature parameter, Sim refers to the similarity matrix between image and text features. Our final distillation loss is defined as:

$$L_{\text{KD}} = \lambda_1 L_{\text{FD}} + \lambda_2 L_{\text{IC}} + \lambda_3 L_{\text{CRD}}, \quad (8)$$

where  $\lambda_1, \lambda_2, \lambda_3$  are hyper-parameters.

### 3.3 Pair Matching (PM) Loss

CLIP models trained on small-scale datasets usually have unsatisfactory zero-shot performance [38]. We argue that one possible reason for this phenomenon is that models trained with fewer data have more difficulties to distinguish image-text pairs that are semantically similar. As a result, we propose to construct an auxiliary hyperplane to help the model determine whether an image-text pair is matched or not. An illustration is shown in Fig. 5.

In particular, we add an extra binary matching task. Given a batch of image-text pairs, we firstly extract the positive image-text pairs and compute their matching logits  $\hat{y}_{I \rightarrow T}^{k(\text{pos})}$  and  $\hat{y}_{T \rightarrow I}^{k(\text{pos})}$ ,  $k = 1, \dots, B$ , given by:

$$\hat{y}_{I \rightarrow T}^{k(\text{pos})} = \text{Linear}(v_k \cdot t_k), \quad (9)$$

$$\hat{y}_{T \rightarrow I}^{k(\text{pos})} = \text{Linear}(t_k \cdot v_k). \quad (10)$$

As for the negative pairs, for each image, we select one negative text according to the image-to-text similarity matrix (one negative text has a high probability to be selected if its embedding is similar to the corresponding image). And the same process is applied to each text. As a result, the negative matching logits are defined as:

$$\hat{y}_{I \rightarrow T}^{k(\text{neg})} = \text{Linear}(v_k \cdot t^{(\text{neg})}), \quad (11)$$

$$\hat{y}_{T \rightarrow I}^{k(\text{neg})} = \text{Linear}(t_k \cdot v^{(\text{neg})}). \quad (12)$$

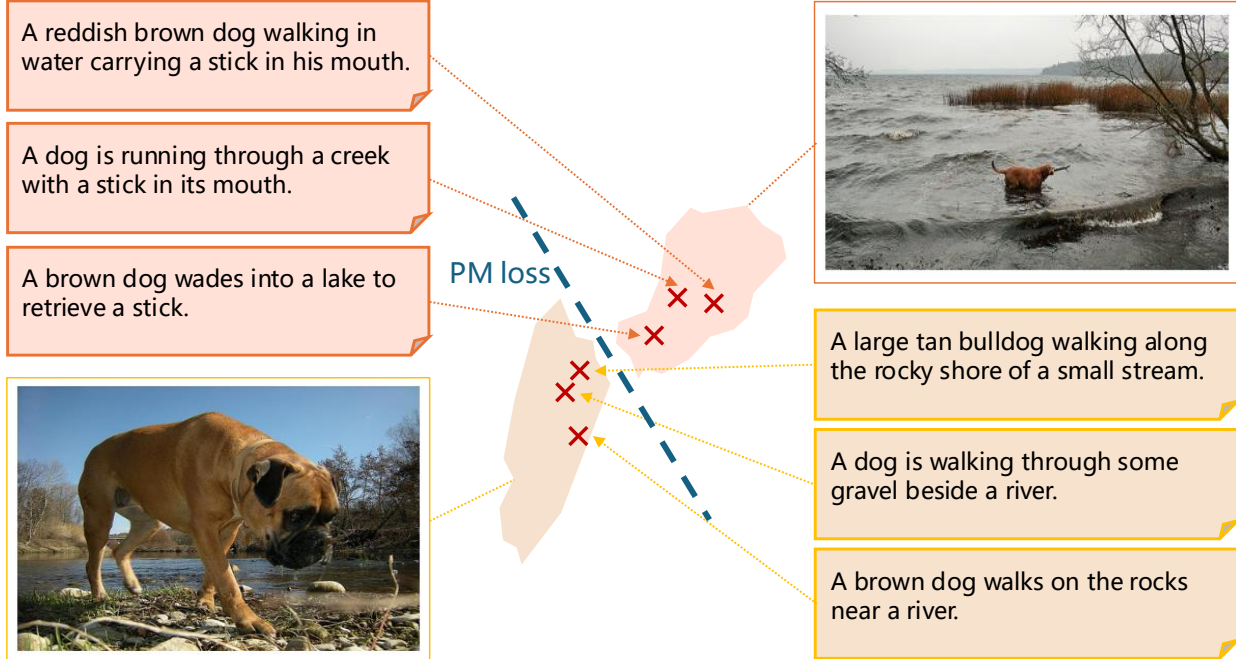


Figure 5: PM loss is proposed to construct an auxiliary hyperplane (blue dashed line) to help the model distinguish semantically similar image-text pairs during training.

Thus, our proposed PM loss is given by:

$$L_{\text{PM}} = \lambda_4(\text{CE}((\hat{y}_{I \rightarrow T}^{k(\text{pos})}, \hat{y}_{I \rightarrow T}^{k(\text{neg})}), \text{label}) + \text{CE}((\hat{y}_{T \rightarrow I}^{k(\text{pos})}, \hat{y}_{T \rightarrow I}^{k(\text{neg})}), \text{label})), \quad (13)$$

and the total loss( $L$ ) is defined as:

$$L = L_{\text{CLIP}} + L_{\text{KD}} + L_{\text{PM}}. \quad (14)$$

### 3.4 CC12M-SYN Dataset

Image-text datasets used to train CLIP models are mostly collected from Internet, containing inherently noisy samples, which are not descriptive enough. When using small-scale datasets, the diversity and quality of data samples becomes even more important. Adding synthetic captions is a cheap but effective way to improve both diversity and quality. We adopt the widely used dataset CC12M [1] and generate multiple synthetic captions for each image in the dataset using coca [43], obtaining CC12M-SYN. Fig. 6 shows some examples with synthetic captions in CC12M-SYN. During training, we randomly select one text from the set of original and synthetic captions. As a result, one sample from CC12M-SYN consists of an image and a synthetic or original caption.

## 4 Experiments

### 4.1 Implementation Details

We adopt a warmup strategy during the first 10000 training iterations. We use AdamW optimizer, and set the batch size to 1536 and weight-decay to 0.1. We train our model for 32 epochs with learning rate 0.001 on an Nvidia RTX3090. In ablation studies, the number of epochs is set to 9. We adopt MobileCLIP-S0 as the teacher for WIKD. For hyper-parameters, we set  $\lambda_1 = 4000$ ,  $\lambda_2 = \lambda_3 = 1$ ,  $\lambda_4 = 0.1$ . Other settings follow CLIP-KD [38].

We evaluate the zero-shot performance on multiple datasets. Specifically, we use ImageNet-1k [4], ImageNet-V2 [29], ImageNet-R [11] and ImageNet-S [35] to evaluate the zero-shot image classification performance. And for zero-shot image-text retrieval, we use MSCOCO [21] and Flickr30k [27]. By default, we report top-1 accuracy (acc1) for image classification and R@1 for image-text retrieval.

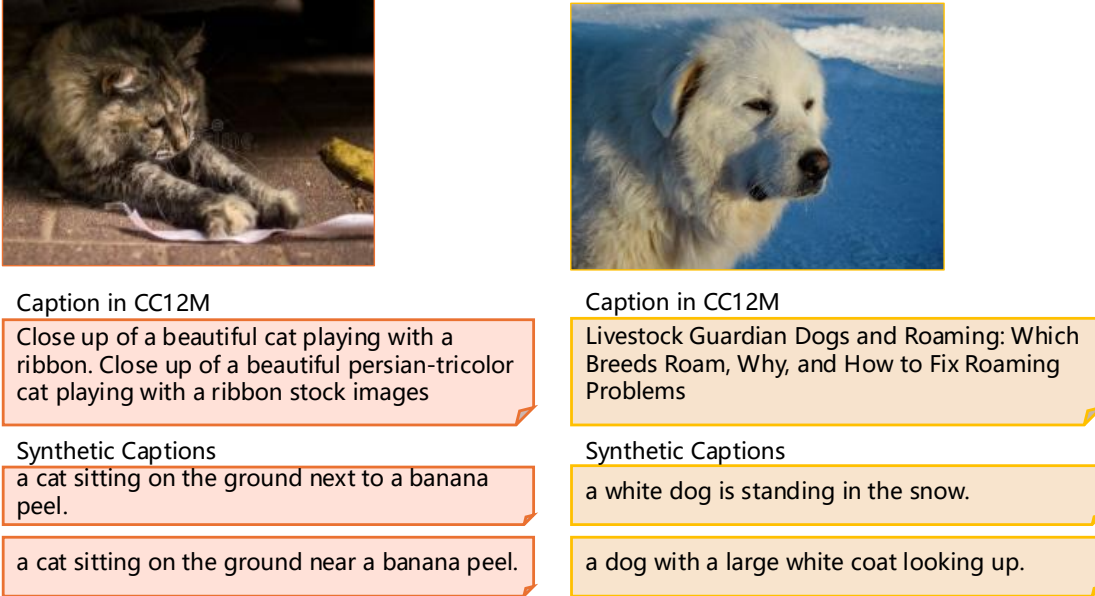


Figure 6: Examples of CC12M-SYN, each sample has one original caption from CC12M and multiple synthetic captions. The synthetic captions are used to provide more descriptions of images, improving both quality and diversity of the dataset.

#### 4.1.1 Data Augmentation.

We apply RandomResizedCrop and RandAugment [2] for image augmentation. We set the scale to (0.08, 1.0) in RandomResizedCrop for a strong augmentation on the original image, and then apply RandAugment on the processed image, which further augments the image by randomly adopting two of the default 31 augmentation methods [2]

### 4.2 Main Results

#### 4.2.1 Zero-shot image-text retrieval.

Table 1 reports the zero-shot image-text retrieval performance on MSCOCO and Flickr30k. Compared with models trained on similar-scale datasets (up to 20M samples), our model outperforms all other works on MSCOCO. As for Flickr30k, our model also achieves the performance of current state-of-the-art model TinyCLIP while using fewer parameters. Compared with models trained on large-scale datasets (400M-1B), our model achieves competitive performance and outperforms many existing works. For example, compared to state-of-the-art MobileCLIP-S0, our model achieves approximately only 1% lower T2I performance while using approximately 3% training samples and 14% fewer image encoder parameters. Moreover, our model outperforms DataComp-B/32, OpenAI-X(except B/16), and LAION-B/32 on both I2T and T2I metrics on both datasets.

#### 4.2.2 Zero-shot image classification on ImageNet.

Table 2 reports the zero-shot classification performances. When compared with models trained on similar-scale datasets, our model outperforms other works on all reported datasets, demonstrating the effectiveness of our methods. As for large-scale datasets, although not as good as the latest state-of-the-art DataComp-B/16, we still achieve some competitive results compared with several existing works.

#### 4.2.3 Inference Speed.

To evaluate the inference speed, we perform simulation experiments on CPU (Intel(R)-Xeon(R)-Silver-4314-CPU@2.40GHz) and compare the average inference speed with the state-of-the-art MobileCLIP series [33]. As shown in table 3, given an input sequence of 1000 images, the processing speed of our model achieves 39.5 images/sec, slightly outperforming state-of-the-art MobileCLIP-S0 (38.2 images/sec). This demonstrates the benefits of adopting SAS-P blocks.

| Name                   | Dataset       | Seen        | Params (M)  |             | MSCOCO      |             | Flickr30k   |             |
|------------------------|---------------|-------------|-------------|-------------|-------------|-------------|-------------|-------------|
|                        |               |             | Samples(B)  | Img         | Txt         | I2T         | T2I         | I2T         |
| DataComp-B/16[7]       | DataComp-1B   | 13          | 86.2        | 63.4        | <b>59.4</b> | <b>42.3</b> | <b>86.3</b> | <b>69.8</b> |
| DataComp-B/32[7]       |               |             | 86.2        | 63.4        | 53.5        | 37.1        | 79.0        | 61.1        |
| MobileCLIP-S0[33]      | DataCompDR-1B | 13          | 11.4        | 42.4        | 58.7        | 40.4        | 85.9        | 67.7        |
| TinyCLIP-63M/32[36]    | LAION-400M    | 15.8        | 86.2        | 63.4        | 55.5        | 37.6        | 83.2        | 64.4        |
| LAION-B/32[30]         |               | (-)         | 86.2        | 63.4        | 53.3        | 35.4        | 79.3        | 62.0        |
| OpenAI-B/16[28]        |               |             | 86.2        | 63.4        | 58.7        | 40.4        | 85.9        | 67.7        |
| OpenAI-B/32[28]        | WIT-400M      | 13          | 86.2        | 63.4        | 50.1        | 30.4        | 78.9        | 58.8        |
| OpenAI-RN50[28]        |               |             | 38.3        | 63.4        | 48.8        | 28.5        | 80.0        | 57.4        |
| RILS-B/16[41]          | LAION-20M     | 0.5         | 86.2        | 37.8        | 32.2        | 25.5        | 45.1        | 34.9        |
| MaskCLIP-B/16[46]      |               |             | 86.2        | 37.8        | 38.5        | 24.8        | 64.9        | 48.1        |
| SLIP-B/16[23]          |               |             | 86.2        | 37.8        | 31.1        | 20.3        | 57.6        | 40.1        |
| TinyCLIP-B/16[36]      | YFCC-15M      | 0.38        | 86.2        | 37.8        | 26.5        | 17.1        | 51.6        | 32.2        |
| TinyCLIP-39M/16[36]    |               |             | 86.2        | 37.8        | 54.9        | 38.9        | <b>84.4</b> | <b>66.7</b> |
| CLIPKD-B/16[38]        |               |             | 86.2        | 37.8        | 25.0        | 24.7        | 54.6        | 56.6        |
| CLIPKD-RN101[38]       |               |             | 56.3        | 37.8        | 25.2        | 25.7        | 57.0        | 55.5        |
| CLIPKD-Swin/T[38]      | CC12M+CC3M    | 0.48        | 27.9        | 21.3        | 28.5        | 28.6        | 62.2        | 60.9        |
| CLIPKD-MobileNetV3[38] |               |             | 2.0         | 21.3        | 17.9        | 16.0        | 42.4        | 42.3        |
| CLIPKD-RN18[38]        |               |             | 11.4        | 21.3        | 21.3        | 19.8        | 47.8        | 47.1        |
| <b>SiCLIP(ours)</b>    | CC12M-SYN     | <b>0.38</b> | <b>9.78</b> | <b>42.4</b> | <b>55.7</b> | <b>39.7</b> | <b>82.0</b> | <b>66.6</b> |

Table 1: Zero-shot retrieval performance compared with existing models.

### 4.3 Ablation Studies

#### 4.3.1 Training Efficiency of CC12M-SYN.

To demonstrate the training efficiency improvement of CC12M-SYN, we train our model separately on CC12M-SYN and CC12M for 20 epochs. We report the average loss curve of first 9 epochs and zero-shot performance on IN-1k and Flickr30k at the last epoch. Fig. 7 reports the loss curves of CC12M and CC12M-SYN, showing that training on CC12M-SYN leads to faster reduction in loss. Table 4 shows that the model trained on CC12M-SYN has better performance on both zero-shot classification and zero-shot image-text retrieval. These results indicate the benefits of synthetic labels for data diversity and quality improvement.

#### 4.3.2 Analysis of WIKD and PM loss.

We explore the effectiveness of WIKD and PM loss by comparing the performance of training without WIKD and PM loss (Baseline), training with WI-only, training with WIKD, and training with both WIKD and PM loss. Results are reported in Table 5. It shows that training with WI-only can provide an improvement on both zero-shot classification and image-text retrieval (+13.0 and +6.1/+0.1 on acc1 of classification and R@1 of retrieval). And when trained with WIKD, the performances will be higher (+25.4 and +15.9/+15.2, respectively). When trained with WIKD and PM loss simultaneously, the model achieves the highest performances. These results evidently support the effectiveness of both WIKD and PM loss.

## 5 Conclusion

In this work, we have proposed a number of techniques to enable training and inference of CLIP models on consumer-level computers while achieving competitive performance. This is critical in bringing the impressive results of foundation models to edge devices. We have reduced the model structure, improving the inference speed. Moreover, we proposed WIKD and PM loss, which have contributed to performance improvement, and can be used in simplifying other models in different domains. Finally, trained on the augmented CC12M-SYN dataset, our model achieved competitive performance compared to existing works despite having fewer parameters and being trained on a smaller dataset.

| Name                   | Dataset       | Seen        | Params (M) |      | IN-1k       | INV2        | IN-R        | IN-S        |
|------------------------|---------------|-------------|------------|------|-------------|-------------|-------------|-------------|
|                        |               |             | Samples(B) | Img  | Img         | Txt         | Img         | Txt         |
| DataComp-B/16[7]       | DataComp-1B   | 13          | 86.2       | 63.4 | <b>73.5</b> | <b>66.0</b> | <b>83.6</b> | <b>60.4</b> |
| DataComp-B/32[7]       |               |             | 86.2       | 63.4 | 69.2        | 60.8        | 78.2        | 56.8        |
| MobileCLIP-S0[33]      | DataCompDR-1B | 13          | 11.4       | 42.4 | 67.8        | 59.9        | 78.6        | 55.5        |
| TinyCLIP-63M/32[36]    |               | 15.8        | 86.2       | 63.4 | 63.9        | 55.7        | 74.1        | 50.8        |
| LAION-B/16[30]         | LAION-400M    | (-)         | 86.2       | 63.4 | 67.0        | 59.4        | 77.8        | 52.3        |
| LAION-B/32[30]         |               |             | 86.2       | 63.4 | 60.2        | 52.3        | 70.8        | 46.5        |
| OpenAI-B/16[28]        |               |             | 86.2       | 63.4 | 68.3        | 61.9        | 77.7        | 48.2        |
| OpenAI-B/32[28]        | WIT-400M      | 13          | 86.2       | 63.4 | 63.3        | 55.9        | 69.3        | 42.3        |
| OpenAI-RN50[28]        |               |             | 38.3       | 63.4 | 59.8        | 52.8        | 60.7        | 35.4        |
| OpenCLIP-RN50[16]      | CC12M         | (-)         | 38.3       | 63.4 | 35.9        | 30.1        | 44.7        | 23.5        |
| OpenCLIP-RN101[16]     | YFCC15M       | (-)         | 56.3       | 63.4 | 34.1        | 29.3        | 26.3        | 8.9         |
| CLIPKD-B/16[38]        |               |             | 86.2       | 37.8 | 37.0        | 32.1        | 48.4        | 26.0        |
| CLIPKD-RN101[38]       |               |             | 56.3       | 37.8 | 36.8        | 31.9        | 49.2        | 26.7        |
| CLIPKD-Swin/T[38]      | CC12M+CC3M    | 0.48        | 27.9       | 21.3 | 40.2        | 34.9        | 51.4        | 28.2        |
| CLIPKD-MobileNetV3[38] |               |             | 2.0        | 21.3 | 27.0        | 23.0        | 30.6        | 14.1        |
| CLIPKD-RN18[38]        |               |             | 11.4       | 21.3 | 31.4        | 26.9        | 39.2        | 20.0        |
| <b>SiCLIP(ours)</b>    | CC12M-SYN     | <b>0.38</b> | 9.78       | 42.4 | <b>58.1</b> | <b>50.7</b> | <b>72.5</b> | <b>47.3</b> |

Table 2: Zero-shot classification performance compared with existing works.

| Model    | SiCLIP(ours) | Mobile-S0  | Mobile-S1   | Mobile-S2   |
|----------|--------------|------------|-------------|-------------|
| Imgs/sec | <b>39.5</b>  | 38.2(-1.3) | 22.2(-17.3) | 18.2(-21.3) |

Table 3: Comparison on inference speed.

## References

- [1] Soravit Changpinyo, Piyush Sharma, Nan Ding, and Radu Soricut. Conceptual 12m: Pushing web-scale image-text pre-training to recognize long-tail visual concepts. In *Proceedings of the IEEE/CVF conference on computer vision and pattern recognition*, pages 3558–3568, 2021.
- [2] Ekin D Cubuk, Barret Zoph, Jonathon Shlens, and Quoc V Le. Randaugment: Practical automated data augmentation with a reduced search space. In *Proceedings of the IEEE/CVF conference on computer vision and pattern recognition workshops*, pages 702–703, 2020.
- [3] Mostafa Dehghani, Stephan Gouws, Oriol Vinyals, Jakob Uszkoreit, and Łukasz Kaiser. Universal transformers. *arXiv preprint arXiv:1807.03819*, 2018.
- [4] Jia Deng, Wei Dong, Richard Socher, Li-Jia Li, Kai Li, and Li Fei-Fei. Imagenet: A large-scale hierarchical image database. In *2009 IEEE conference on computer vision and pattern recognition*, pages 248–255. Ieee, 2009.
- [5] Alexey Dosovitskiy, Lucas Beyer, Alexander Kolesnikov, Dirk Weissenborn, Xiaohua Zhai, Thomas Unterthiner, Mostafa Dehghani, Matthias Minderer, Georg Heigold, Sylvain Gelly, et al. An image is worth 16x16 words: Transformers for image recognition at scale. *arXiv preprint arXiv:2010.11929*, 2020.
- [6] Alex Fang, Albin Madappally Jose, Amit Jain, Ludwig Schmidt, Alexander Toshev, and Vaishaal Shankar. Data filtering networks. *arXiv preprint arXiv:2309.17425*, 2023.
- [7] Samir Yitzhak Gadre, Gabriel Ilharco, Alex Fang, Jonathan Hayase, Georgios Smyrnis, Thao Nguyen, Ryan Marten, Mitchell Wortsman, Dhruba Ghosh, Jieyu Zhang, et al. Datacomp: In search of the next generation of multimodal datasets. *Advances in Neural Information Processing Systems*, 36, 2024.
- [8] Anmol Gulati, James Qin, Chung-Cheng Chiu, Niki Parmar, Yu Zhang, Jiahui Yu, Wei Han, Shibo Wang, Zhengdong Zhang, Yonghui Wu, et al. Conformer: Convolution-augmented transformer for speech recognition. *arXiv preprint arXiv:2005.08100*, 2020.

| Dataset (Storage) | IN-1k<br>(T→I)    | Flickr30k<br>(I→T) |
|-------------------|-------------------|--------------------|
| CC12M (235G)      | 53.4              | 57.4               |
| CC12M-SYN (236G)  | <b>54.5(+1.1)</b> | <b>65.1(+7.7)</b>  |
|                   | <b>78.0(+4.5)</b> |                    |

Table 4: CC12M-SYN vs CC12M.

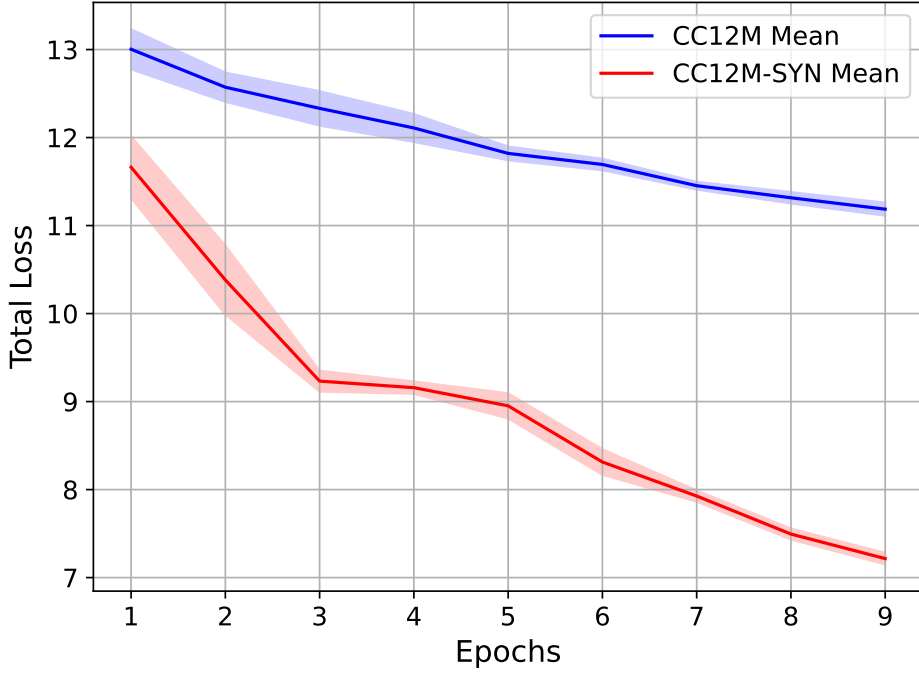


Figure 7: Comparison of training efficiency between CC12M and CC12M-SYN dataset.

- [9] Jianyuan Guo, Kai Han, Han Wu, Yehui Tang, Xinghao Chen, Yunhe Wang, and Chang Xu. Cmt: Convolutional neural networks meet vision transformers. In *Proceedings of the IEEE/CVF conference on computer vision and pattern recognition*, pages 12175–12185, 2022.
- [10] Bobby He and Thomas Hofmann. Simplifying transformer blocks. In *The Twelfth International Conference on Learning Representations*, 2024.
- [11] Dan Hendrycks, Steven Basart, Norman Mu, Saurav Kadavath, Frank Wang, Evan Dorundo, Rahul Desai, Tyler Zhu, Samyak Parajuli, Mike Guo, et al. The many faces of robustness: A critical analysis of out-of-distribution generalization. In *Proceedings of the IEEE/CVF international conference on computer vision*, pages 8340–8349, 2021.
- [12] Steven M Hernandez, Ding Zhao, Shaojin Ding, Antoine Bruguier, Rohit Prabhavalkar, Tara N Sainath, Yanzhang He, and Ian McGraw. Sharing low rank conformer weights for tiny always-on ambient speech recognition models. In *ICASSP 2023-2023 IEEE International Conference on Acoustics, Speech and Signal Processing (ICASSP)*, pages 1–5. IEEE, 2023.
- [13] Geoffrey Hinton, Oriol Vinyals, and Jeff Dean. Distilling the knowledge in a neural network. *arXiv preprint arXiv:1503.02531*, 2015.
- [14] Qibin Hou, Ming-Ming Cheng, Xiaowei Hu, Ali Borji, Zhuowen Tu, and Philip HS Torr. Deeply supervised salient object detection with short connections. In *Proceedings of the IEEE conference on computer vision and pattern recognition*, pages 3203–3212, 2017.
- [15] Edward J Hu, Yelong Shen, Phillip Wallis, Zeyuan Allen-Zhu, Yuanzhi Li, Shean Wang, Lu Wang, and Weizhu Chen. Lora: Low-rank adaptation of large language models. *arXiv preprint arXiv:2106.09685*, 2021.
- [16] Gabriel Ilharco, Mitchell Wortsman, Ross Wightman, Cade Gordon, Nicholas Carlini, Rohan Taori, Achal Dave, Vaishaal Shankar, Hongseok Namkoong, John Miller, et al. Openclip repository, 2021.

| Method   | IN-1k              |                    | Flickr30k          |       |
|----------|--------------------|--------------------|--------------------|-------|
|          |                    | (T→I)              |                    | (I→T) |
| Baseline | 27.0               | 49.1               | 60.9               |       |
| WI       | 40.0(+13.0)        | 55.2(+6.1)         | 61.0(+0.1)         |       |
| WIKD     | 52.4(+25.4)        | 62.8(+13.7)        | 76.1(+15.2)        |       |
| WIKD+PM  | <b>55.0(+28.0)</b> | <b>64.7(+15.6)</b> | <b>79.1(+18.2)</b> |       |

Table 5: Analysis of WIKD and PM loss.

- [17] Andrew Jaegle, Felix Gimeno, Andy Brock, Oriol Vinyals, Andrew Zisserman, and Joao Carreira. Perceiver: General perception with iterative attention. In *International conference on machine learning*, pages 4651–4664. PMLR, 2021.
- [18] Zhengfeng Lai, Haotian Zhang, Wentao Wu, Haoping Bai, Aleksei Timofeev, Xianzhi Du, Zhe Gan, Jiulong Shan, Chen-Nee Chuah, Yinfei Yang, et al. From scarcity to efficiency: Improving clip training via visual-enriched captions. *arXiv preprint arXiv:2310.07699*, 2023.
- [19] Junnan Li, Dongxu Li, Caiming Xiong, and Steven Hoi. Blip: Bootstrapping language-image pre-training for unified vision-language understanding and generation. In *International conference on machine learning*, pages 12888–12900. PMLR, 2022.
- [20] Yangguang Li, Feng Liang, Lichen Zhao, Yufeng Cui, Wanli Ouyang, Jing Shao, Fengwei Yu, and Junjie Yan. Supervision exists everywhere: A data efficient contrastive language-image pre-training paradigm. *arXiv preprint arXiv:2110.05208*, 2021.
- [21] Tsung-Yi Lin, Michael Maire, Serge Belongie, James Hays, Pietro Perona, Deva Ramanan, Piotr Dollár, and C Lawrence Zitnick. Microsoft coco: Common objects in context. In *Computer Vision–ECCV 2014: 13th European Conference, Zurich, Switzerland, September 6–12, 2014, Proceedings, Part V 13*, pages 740–755. Springer, 2014.
- [22] Ze Liu, Yutong Lin, Yue Cao, Han Hu, Yixuan Wei, Zheng Zhang, Stephen Lin, and Baining Guo. Swin transformer: Hierarchical vision transformer using shifted windows. In *Proceedings of the IEEE/CVF international conference on computer vision*, pages 10012–10022, 2021.
- [23] Norman Mu, Alexander Kirillov, David Wagner, and Saining Xie. Slip: Self-supervision meets language-image pre-training. In *European conference on computer vision*, pages 529–544. Springer, 2022.
- [24] Xueyan Niu, Bo Bai, Lei Deng, and Wei Han. Beyond scaling laws: Understanding transformer performance with associative memory. *arXiv preprint arXiv:2405.08707*, 2024.
- [25] Lorenzo Noci, Chunling Li, Mufan Li, Bobby He, Thomas Hofmann, Chris J Maddison, and Dan Roy. The shaped transformer: Attention models in the infinite depth-and-width limit. *Advances in Neural Information Processing Systems*, 36, 2024.
- [26] Zizheng Pan, Bohan Zhuang, Haoyu He, Jing Liu, and Jianfei Cai. Less is more: Pay less attention in vision transformers. In *Proceedings of the AAAI Conference on Artificial Intelligence*, volume 36, pages 2035–2043, 2022.
- [27] Bryan A Plummer, Liwei Wang, Chris M Cervantes, Juan C Caicedo, Julia Hockenmaier, and Svetlana Lazebnik. Flickr30k entities: Collecting region-to-phrase correspondences for richer image-to-sentence models. In *Proceedings of the IEEE international conference on computer vision*, pages 2641–2649, 2015.
- [28] Alec Radford, Jong Wook Kim, Chris Hallacy, Aditya Ramesh, Gabriel Goh, Sandhini Agarwal, Girish Sastry, Amanda Askell, Pamela Mishkin, Jack Clark, et al. Learning transferable visual models from natural language supervision. In *International conference on machine learning*, pages 8748–8763. PMLR, 2021.
- [29] Benjamin Recht, Rebecca Roelofs, Ludwig Schmidt, and Vaishaal Shankar. Do imagenet classifiers generalize to imagenet? In *International conference on machine learning*, pages 5389–5400. PMLR, 2019.
- [30] Christoph Schuhmann, Romain Beaumont, Richard Vencu, Cade Gordon, Ross Wightman, Mehdi Cherti, Theo Coombes, Aarush Katta, Clayton Mullis, Mitchell Wortsman, et al. Laion-5b: An open large-scale dataset for training next generation image-text models. *Advances in Neural Information Processing Systems*, 35:25278–25294, 2022.
- [31] Sainbayar Sukhbaatar, Edouard Grave, Guillaume Lample, Herve Jegou, and Armand Joulin. Augmenting self-attention with persistent memory. *arXiv preprint arXiv:1907.01470*, 2019.

- [32] Pavan Kumar Anasosalu Vasu, James Gabriel, Jeff Zhu, Oncel Tuzel, and Anurag Ranjan. Fastvit: A fast hybrid vision transformer using structural reparameterization. In *Proceedings of the IEEE/CVF International Conference on Computer Vision*, pages 5785–5795, 2023.
- [33] Pavan Kumar Anasosalu Vasu, Hadi Pouransari, Fartash Faghri, Raviteja Vemulapalli, and Oncel Tuzel. Mobileclip: Fast image-text models through multi-modal reinforced training. In *Proceedings of the IEEE/CVF Conference on Computer Vision and Pattern Recognition*, pages 15963–15974, 2024.
- [34] Ashish Vaswani, Noam Shazeer, Niki Parmar, Jakob Uszkoreit, Llion Jones, Aidan N Gomez, Łukasz Kaiser, and Illia Polosukhin. Attention is all you need. *Advances in neural information processing systems*, 30, 2017.
- [35] Haohan Wang, Songwei Ge, Zachary Lipton, and Eric P Xing. Learning robust global representations by penalizing local predictive power. *Advances in Neural Information Processing Systems*, 32, 2019.
- [36] Kan Wu, Houwen Peng, Zhenghong Zhou, Bin Xiao, Mengchen Liu, Lu Yuan, Hong Xuan, Michael Valenzuela, Xi Stephen Chen, Xinggang Wang, et al. Tinyclip: Clip distillation via affinity mimicking and weight inheritance. In *Proceedings of the IEEE/CVF International Conference on Computer Vision*, pages 21970–21980, 2023.
- [37] Zhe Wu, Li Su, and Qingming Huang. Cascaded partial decoder for fast and accurate salient object detection. In *Proceedings of the IEEE/CVF conference on computer vision and pattern recognition*, pages 3907–3916, 2019.
- [38] Chuanguang Yang, Zhulin An, Libo Huang, Junyu Bi, Xinqiang Yu, Han Yang, Boyu Diao, and Yongjun Xu. Clip-kd: An empirical study of clip model distillation. In *Proceedings of the IEEE/CVF Conference on Computer Vision and Pattern Recognition*, pages 15952–15962, 2024.
- [39] Jianwei Yang, Chunyuan Li, Pengchuan Zhang, Bin Xiao, Ce Liu, Lu Yuan, and Jianfeng Gao. Unified contrastive learning in image-text-label space. In *Proceedings of the IEEE/CVF Conference on Computer Vision and Pattern Recognition*, pages 19163–19173, 2022.
- [40] Kaicheng Yang, Jiankang Deng, Xiang An, Jiawei Li, Ziyong Feng, Jia Guo, Jing Yang, and Tongliang Liu. Alip: Adaptive language-image pre-training with synthetic caption. In *Proceedings of the IEEE/CVF International Conference on Computer Vision*, pages 2922–2931, 2023.
- [41] Shusheng Yang, Yixiao Ge, Kun Yi, Dian Li, Ying Shan, Xiaohu Qie, and Xinggang Wang. Rils: Masked visual reconstruction in language semantic space. In *Proceedings of the IEEE/CVF Conference on Computer Vision and Pattern Recognition*, pages 23304–23314, 2023.
- [42] Lewei Yao, Runhui Huang, Lu Hou, Guansong Lu, Minzhe Niu, Hang Xu, Xiaodan Liang, Zhenguo Li, Xin Jiang, and Chunjing Xu. Filip: Fine-grained interactive language-image pre-training. *arXiv preprint arXiv:2111.07783*, 2021.
- [43] Jiahui Yu, Zirui Wang, Vijay Vasudevan, Legg Yeung, Mojtaba Seyedhosseini, and Yonghui Wu. Coca: Contrastive captioners are image-text foundation models. *arXiv preprint arXiv:2205.01917*, 2022.
- [44] Weihao Yu, Mi Luo, Pan Zhou, Chenyang Si, Yichen Zhou, Xinchao Wang, Jiashi Feng, and Shuicheng Yan. Metaformer is actually what you need for vision. In *Proceedings of the IEEE/CVF conference on computer vision and pattern recognition*, pages 10819–10829, 2022.
- [45] Xiaohua Zhai, Basil Mustafa, Alexander Kolesnikov, and Lucas Beyer. Sigmoid loss for language image pre-training. In *Proceedings of the IEEE/CVF International Conference on Computer Vision*, pages 11975–11986, 2023.
- [46] Chong Zhou, Chen Change Loy, and Bo Dai. Extract free dense labels from clip. In *European Conference on Computer Vision*, pages 696–712. Springer, 2022.